Journal of Digital Health and Advanced Biomaterials
e-ISSN 3086-5972 Diamond Open Access journal.jdhab.org

From facial surface acquisition to digital orthopedic support

Biomechanical rationale, clinical proof-of-concept, and validation agenda for a patient-specific Digital Sky Hook

Lisandro Gonçalves, DDS, MSc[1,2]; Hélio Hissashi Terada, DDS, MSc, PhD[3]

[1] Journal of Digital Health and Advanced Biomaterials, Maringá, Paraná, Brazil.
[2] LifeDent Esthetic Clinic, Maringá, Paraná, Brazil.
[3] Department of Dentistry, State University of Maringá, Maringá, Paraná, Brazil.
Co-author ORCID: 0000-0002-5869-5103

editor@jdhab.org • ORCID 0009-0004-8140-2876

Published 23 May 2026 • pp. 55–69 • DOI 10.67463/d329dc10

ABSTRACT

Objective: To document the clinical-technical proof-of-concept of a patient-specific Digital Sky Hook for maxillary protraction, emphasizing how non-contact facial acquisition and additive manufacturing may stabilize the extraoral support interface for classical chin-supported mechanics. **Methods:** Two clinical-technical applications were considered. The index case, a growing female patient with skeletal Class III malocclusion and maxillary deficiency, was described in detail because complete acquisition, design, fabrication, delivery, seating assessment, and follow-up documentation were available. A second ongoing-use application documented procedural repeatability without statistical or comparative outcome claims. **Results:** Three design and printing iterations were required before standardizing the index appliance. The finalized framework showed passive seating, required no hydrocolloid foam or compensatory lining, and was used for 12 to 14 hours per day over an 8-month period without clinically relevant soft-tissue adverse events. Exploratory comparison with a conventional support showed border discrepancies of approximately 2.0 mm superiorly and 2.5 mm inferiorly. The workflow was reproduced in a second patient who received the appliance and remained in active use. **Conclusion:** This Methods / Technical Note / Validation Study establishes the feasibility and procedural repeatability of a scan-derived, patient-specific chin-support interface for a classical Sky Hook-type maxillary protraction system. The workflow reduced dependence on facial molding, enabled passive seating without compensatory lining in the index case, and provides a traceable platform for metrological, mechanical, pressure-distribution, and prospective clinical validation.

KEYWORDS CAD/CAM; facial photogrammetry; Class III malocclusion; maxillary protraction; additive manufacturing; patient-specific device; digital orthodontics; orthopedic appliance

EXPLORE Article text References Online record

Article record

Canonical citation
Gonçalves L, Terada HH. From facial surface acquisition to digital orthopedic support: Biomechanical rationale, clinical proof-of-concept, and validation agenda for a patient-specific Digital Sky Hook. J Digit Health Adv Biomater. 2026;1(1):55–69. https://doi.org/10.67463/d329dc10.

Assessment Peer-reviewed

Introduction

Skeletal Class III malocclusion associated with maxillary deficiency remains one of the most demanding problems in interceptive orthodontics. In growing patients, maxillary protraction is not simply an appliance choice; it is a biomechanical strategy in which diagnosis, skeletal maturity, vertical facial pattern, transverse correction, intraoral anchorage, extraoral support stability, force direction, and patient cooperation must act as a coordinated system[1,4,12]. The historical source of the chin-supported anterior traction family is John H. Hickham's orthodontic anterior traction appliance.

Hickham's design combined a chin cup, vertical traction arms, posterior stabilizing arms, elastic traction, and a resultant force vector intended to keep the support seated against displacement during mandibular and head movement[2–4]. In contemporary clinical and commercial language, the term NOLA/Hickham may appear in association with prefabricated protraction headgear, but this nomenclature should not obscure Hickham's role as the originator of the mechanical concept. In this manuscript, Sky Hook is used as the clinical and geometric descriptor of the elevated extraoral hook architecture, whereas Digital Sky Hook identifies the patient-specific digital workflow used to obtain and reproduce the support interface. This distinction is central to the present article.

The Digital Sky Hook is not proposed as a new biological mechanism for maxillary protraction, nor as a mere copy of Hickham's appliance. The preserved principle is classical chin-supported anterior traction; the introduced modification is the patient-specific support-interface pathway, obtained through facial surface acquisition, mesh-based planning, STL-oriented design, additive manufacturing, and file-based documentation. The chin support is therefore not a secondary comfort accessory.

It is part of the force-transmitting system. Its seating behavior influences the position of the anterior hooks, the clearance from the lower lip, the effectiveness of the lateral stabilizing arms, the action of the occipital headcap, and the consistency of the elastic line of action. If the base rocks, slides, or compresses soft tissues unevenly, the intended relationship among chin support, maxillary anchorage, elastic pathway, and stabilizing headcap may change during function[3–5,8]. Analog fabrication of individualized chin-supported appliances remains clinically familiar, but it has an inherent limitation: the soft-tissue surface that must later distribute orthopedic load is recorded by a contact procedure that may compress or distort it.

Impression pressure, material weight, cast-transfer error, and manual finishing can all affect the final geometry. A mismatch at the support interface may produce localized pressure concentration, need for compensatory lining, instability during mandibular function, and loss of control over the intended traction geometry. The present article therefore documents the clinical and methodological proof-of-concept of a patient-specific Digital Sky Hook framework.

It evaluates whether non-contact facial acquisition, STL-based planning, additive manufacturing, and hybrid laboratory assembly can preserve support-interface adaptation while maintaining the biomechanical logic of chin-supported maxillary protraction. Therefore, the present study does not propose a new biological mechanism for maxillary protraction, but a digitally traceable and metrically inspectable workflow for engineering a patient-specific chin-support interface within a classical orthopedic force system.

Materials and methods

Study design and methodological scope

This Methods / Technical Note / Validation Study documents a complete design-to-delivery workflow and two clinical-technical applications of a patient-specific, digitally planned support interface integrated into an established chin-supported maxillary protraction system. The index application is reported in detail, and an additional ongoing-use application is included to support procedural repeatability of the workflow.

The emphasis remains technical feasibility, fabrication control, seating behavior, clinical usability, and traceability of the support-interface pathway. The study therefore evaluates the Digital Sky Hook as a proof-of-concept platform for support-interface individualization.

The relevant endpoints are support-interface adaptation, seating stability, soft-tissue tolerance, digital traceability, and the validation pathway required to convert this technical innovation into measurable biomechanical and clinical evidence. The workflow was documented in two clinical-technical applications.

The index case was selected for full reporting because the complete pathway was available, including facial acquisition, digital planning, additive manufacturing, laboratory assembly, delivery, support-interface assessment, and clinical follow-up. A second patient also received the appliance and remained in active use at the time of manuscript preparation.

This additional application was included to document procedural repeatability of the workflow, not to estimate population-level treatment effects or compare clinical outcomes.

Orthodontic baseline and clinical indication

The index clinical application involved a growing female patient aged 10 years and 2 months. The patient presented with a skeletal Class III pattern characterized by a concave facial profile, mandibular prominence, brachyfacial/hypodivergent vertical pattern, and maxillary transverse deficiency.

Cephalometric values included SNA of 81 degrees, SNB of 83 degrees, ANB of -2 degrees, Wits appraisal of -4 mm, NAP of -6 degrees, FMA of 19 degrees, SN-GoGn of 27 degrees, and Y-axis of 62 degrees. The molar relationship was Class I in a skeletal Class III context, with dental compensation involving proclination/protrusion of the maxillary incisors and verticalization/retrusion of the mandibular incisors.

The clinical indication for the Digital Sky Hook was based on the need for individualized extraoral support during maxillary protraction therapy, with particular attention to stability of the chin-support interface, vertical control, patient tolerance, and preservation of the intended traction geometry. Rapid palatal expansion served as the intraoral anchorage platform for the Class III elastic traction pathway.

The index patient had previous experience with a conventionally obtained extraoral support and later underwent digitally planned support iterations; this within-patient experience informed the technical development, but it was not treated as comparative clinical-efficacy evidence.

Facial acquisition and digital file handling

Facial surface acquisition was performed with the patient at rest, without intentional facial expression and without external compression of the mentolabial or symphyseal soft tissues. The facial record was obtained using a Cloner facial scanning booth (dOne 3D, Ribeirao Preto, Brazil), based on multi-camera photogrammetry with cameras embedded in adjustable arcs and supports around the patient. The approximate working distance was 55 cm from the patient's face, depending on the position of the cameras within the booth.

The acquisition time was approximately 0.4 seconds. Scanner calibration was performed according to the manufacturer-guided protocol using a dedicated calibration target with geometric markings. The software-guided calibration sequence allowed alignment of the integrated cameras and adjustment of acquisition parameters before clinical capture.

Scan acceptance criteria were also standardized. The patient was seated in natural head posture, with relaxed lips, no intentional smile, no active mandibular protrusion, and no external pressure over the mentolabial or symphyseal soft tissues. Captures were accepted only when the lower facial third, lower lip, mentolabial sulcus, pogonion region, and lateral chin contours were continuous enough to support mesh delimitation.

When motion blur, incomplete lower-face capture, texture/geometry mismatch, or surface holes affected the support region, the scan was repeated before device design. These criteria were used because the chin-support base was derived directly from the facial surface record. The original data package included geometry and texture-related files, including OBJ, MTL, and JPEG components. The working mesh was subsequently handled in STL format for device design and manufacturing. Original records, converted files, intermediate design versions, prototypes, and final manufacturing files were preserved as distinct workflow stages to maintain digital traceability. Because facial surface files constitute patient-specific biometric data, original identifiable facial files were not considered suitable for open public sharing.

The conversion from the original textured facial record to STL was performed because STL is widely supported by mesh-editing, slicing, and additive-manufacturing software. Color and texture information were not required for the support-interface geometry and were not used for fabrication. Scale and units were checked during file import and export by maintaining the original coordinate scale and by verifying the approximate anatomical dimensions of the lower facial segment before design.

Mesh preparation was limited to removal of irrelevant peripheral artifacts, local smoothing when needed, and correction of defects that interfered with support-region delimitation; no global deformation of the menton support surface was intentionally introduced. Digital-file governance followed a versioned workflow. Original identifiable facial files, converted working meshes, intermediate design files, prototype versions, final manufacturing files, and screenshots used for documentation were stored as separate stages.

Access to identifiable facial files was restricted to the clinical/ design team. De-identified screenshots and workflow documentation may be shared for scientific review, whereas original facial biometric files are not publicly distributed.

Digital support design and fabrication controls

The support region was delineated directly on the resting facial mesh in a mesh-editing environment. The design goal was not to create a new protraction mechanics, but to translate the classical Sky Hook architecture into a patient-specific support interface derived from uncompressed facial anatomy. The initial support plate and frontal plate were generated using selected surface extrusion, duplication, and Boolean operations.

Negative retention tracks were incorporated into the design to guide the placement of the metallic framework. These L-shaped channels were intended to improve wire accommodation and reduce freehand variability during laboratory assembly. In practical terms, the facial mesh was first used to delimit the intended mental support area.

The first plate (P1) was generated from this selected support region by surface extrusion/offset of approximately 1.5 mm, creating the patient-contact support component. A duplicate of this geometry was preserved as a backup before subsequent Boolean operations. The frontal component (P2) was generated from the P1 geometry by selecting the external surface, creating an additional approximately 1.5-mm extrusion, and subtracting the initial component to create a complementary layer.

Border smoothing and finishing were planned to avoid sharp edges at the superior, inferior, and lateral margins. The L-shaped retention channels were designed as negative spaces for accommodation of the chromiumnickel wire framework. Their position and emergence angles were determined by the orthodontic objective and by the CAD operator in communication with the clinician, using the facial contour, lip clearance, planned elastic path, and mechanical feasibility of wire insertion as constraints.

The channels were intended to provide passive accommodation and mechanical retention after laboratory assembly, while still allowing final wire bending and acrylic union to be performed by the technician. Because this was a clinical-technical proofof-concept, channel geometry was treated as a controlled design decision rather than as a fully automated parameter. The workflow remained hybrid.

Digital planning and printed geometry guided the support base and wireretention architecture, whereas wire bending, wire insertion, acrylic union, finishing, polishing, and clinical adjustment remained operator-dependent steps. To support manufacturing consistency, the additivemanufacturing protocol was standardized before clinical delivery. The final components were prepared in FlashPrint and manufactured by DLP using a FlashForge Hunter printer and transparent Cosmos SG biocompatible resin, indicated for surgical guides.

The components were oriented vertically, approximately 90 degrees relative to the build platform, using an automatic support strategy. Layer exposure was approximately 2 seconds at 100% light intensity according to the printer/resin workflow used in the case. The vertical build orientation was selected to reduce broad unsupported horizontal surfaces and to preserve the curvature of the support interface during printing and post-processing.

Automatic support generation was used, followed by manual inspection of support placement to avoid support scars on the primary patient-contact surface whenever possible. Exposure parameters were kept constant within the selected printer-resin workflow, including approximately 2 seconds per layer and 100% light-intensity setting, followed by the resin-compatible post-curing protocol described below. Three design and printing iterations were performed before standardizing the final configuration.

No visible deformation or warpage compromising clinical seating was observed in the final printed components. Postprocessing followed a controlled sequence: alcoholbased washing for up to 10 minutes, complete drying, ultraviolet post-curing for 10 minutes in a FlashForge FC-1 unit, support removal, finishing, mechanical polishing, and visual inspection. When residual surface opacity was observed after drying, the surface was gently brushed with a soft brush moistened with clean alcohol and dried with compressed air.

The resin pathway was also documented from a regulatory-traceability perspective. The transparent biocompatible resin was selected from a supplier operating under Brazilian sanitary regulatory authorization. In Brazil, the Autorização de Funcionamento de Empresa (AFE) is issued by Anvisa and certifies that the company is legally authorized to perform activities involving products subject to sanitary surveillance.

This authorization supports regulatory traceability of the supplier/material pathway, but it does not replace device-specific testing for prolonged extraoral skin contact. For that reason, the appliance was finished, polished, cleaned, and clinically monitored as a prolonged-contact extraoral device. The patient/caregiver received routine maintenance instructions, including removal of visible debris after use, gentle cleaning of the appliance surfaces, and surface disinfection compatible with the resin, acrylic, and metallic components.

During follow-up, the device was inspected for surface roughness, cracks, odor retention, discoloration, material degradation, wire loosening, tissue irritation, erythema, pressure marks, discomfort, and need for adjustment. The metallic framework was adapted by the laboratory technician into the digitally planned negative channels. The printed components were then joined using chemically activated acrylic resin.

Final quality control was based on visual inspection, fitting of the metallic framework, absence of visible deformation, and clinical passive seating assessment.

Clinical delivery, traction configuration, and monitoring

The final appliance was delivered clinically after verification of passive seating and absence of excessive pressure on the mentolabial and submandibular regions. Class III elastic traction was performed using 5/16-inch elastics connected from the anterior hooks of the extraoral framework to the hooks of the maxillary intraoral anchorage unit.

Elastics were replaced daily to reduce force decay associated with elongation, thermal exposure, moisture, and fatigue. No fixed numerical force value was reported as a continuously maintained load, because the effective force delivered by elastics depends on brand, elastic category, degree of elongation, hook-to-hook distance, intraoral moisture, time in function, and replacement interval.

Instead, the traction protocol was documented in terms of elastic configuration, daily replacement, clinical adjustment, patient tolerance, soft-tissue response, and biomechanical control. Biomechanical adjustment was interpreted according to the moment relationship $M = F \times d$, in which the generated moment depends on the applied force and the perpendicular distance between the line of action and the relevant center of resistance or rotation.

The occipital headcap and lateral wire framework were used to stabilize the extraoral assembly, maintain lip clearance, and limit excessive displacement of the chin support during function. The patient was instructed to use the appliance for 12 to 14 hours per day during the active clinical-use period.

Follow-up monitoring included assessment of seating stability, soft-tissue tolerance, pressure marks, erythema, pain, need for compensatory lining, device integrity, and patient-reported tolerance. The appliance was also evaluated for fracture, visible deformation, instability, or need for clinical adjustment.

Scan-based CAD-to-as-built congruence assessment

After identification of the original nominal digital design files, the patient-contact and frontal support components (P1/P2) were imported as the nominal design reference. The clinically used chin-support component was also scanned after fabrication and clinical use to document the as-built surface geometry. Tables 1 and 2 summarize baseline context and workflow parameters.

Table 1. Anonymized orthodontic baseline and rationale for individualized extraoral protraction support.

Domain	Finding	Clinical relevance
Patient context	Female patient; 10 years and 2 months; growing patient	Age and growth status compatible with interceptive orthopedic management
Facial pattern	Concave profile, mandibular prominence, facial symmetry, lip seal	Supports skeletal Class III characterization and need for orthopedic assessment
Vertical pattern	Brachyfacial/hypodivergent pattern; FMA 19°, SN-GoGn 27°, Y-axis 62°	Requires attention to vertical control and rotational side effects
Sagittal skeletal values	SNA 81°, SNB 83°, ANB -2°, Wits -4 mm, NAP -6°	Consistent with skeletal Class III discrepancy and maxillomandibular imbalance
Dental pattern	Class I molar relationship in a skeletal Class III context; upper incisors proclined/protruded; lower incisors compensated/retruded/verticalized	Indicates dental compensation and the need to distinguish support-interface findings from treatment-effectiveness claims
Transverse problem	Maxillary constriction/atresia; rapid palatal expansion used or planned as intraoral anchorage platform	Provides internal anchorage for Class III elastic traction pathway
Previous orthopedic context	Prior facemask traction and maxillary expander reported in clinical record	Supports clinical relevance of alternative extraoral support design

Source: Authors' synthesis based on the de-identified diagnostic records described in this study.

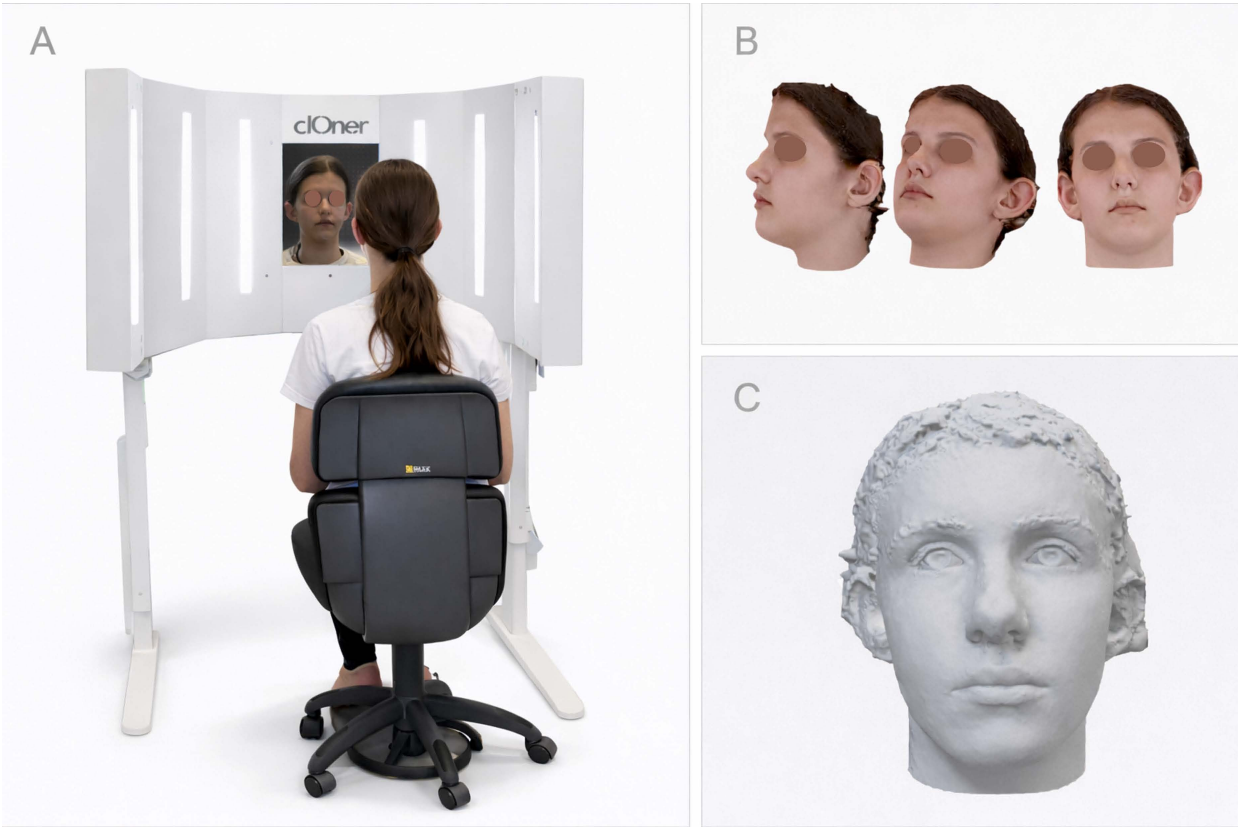
Table 2. Core technical parameters of the Digital Sky Hook workflow.

Technical domain	Parameter documented in the manuscript	Purpose in the workflow
Facial acquisition	Non-contact multi-camera facial capture at rest; relaxed lips; no external compression; manufacturer-guided calibration and acceptance criteria for scan quality.	Records the menton support area without impression pressure and defines the anatomical substrate for design.
File handling	Original geometry/texture package preserved; working geometry converted to STL with scale/units maintained; texture data not used for support fabrication.	Allows mesh editing, slicing and additive manufacturing while preserving traceability of source files.
Mesh and CAD design	Manual delimitation of the menton support region; P1/P2 construction by selected surface extrusion, duplication and Boolean operations.	Transforms the resting facial surface into a patient-specific support interface.
Wire-retention channels	L-shaped negative channels planned for a 1.20-mm CrNi wire framework, with final angulation and dimensions guided by orthodontic and laboratory expertise.	Guides wire placement and reduces freehand variability while preserving necessary operator judgment.
Additive manufacturing	FlashPrint slicing; FlashForge Hunter DLP printing; Cosmos SG transparent biocompatible resin; vertical orientation at approximately 90 degrees; automatic supports; approximately 2 s exposure per layer at 100% light intensity.	Documents the manufacturing layer used to fabricate the support components.
Post-processing and finishing	Alcohol-based washing up to 10 minutes, complete drying, ultraviolet post-curing for 10 minutes, support removal, finishing, polishing, and clinical inspection.	Reduces surface residues and prepares the device for clinical handling and soft-tissue contact.
Material and regulatory traceability	Resin selected from a supplier operating under Brazilian sanitary authorization (Anvisa AFE), interpreted as company/material-pathway traceability rather than device-specific proof of prolonged skin-contact safety.	Supports responsible material selection while preserving the need for future skin-contact and pressure validation.
Digital governance	Versioned storage of original facial files, converted meshes, intermediate design stages, prototypes, and final manufacturing files, with restrictions on sharing identifiable biometric data.	Supports auditability, controlled remanufacturing, and patient privacy.

Source: Developed by the authors from the documented Digital Sky Hook workflow.

An exploratory best-fit/ICP alignment was then performed between the scanned as-built component and the nominal P1/P2 design surface. The purpose of this analysis was to provide a first quantitative layer of exploratory CAD-to-as-built surface-deviation assessment, while preserving the distinction between validation-oriented research metrology and certification-level dimensional inspection.

Figure 1 — Non-contact facial surface acquisition and patient-specific support planning



Source: Authors' clinical and technical archive; de-identified record reproduced with authorization.
(A) Facial surface acquisition setup used to capture the lower facial third under resting conditions, without external compression of the mentolabial or symphyseal soft tissues. (B) Three-dimensional facial record used as the anatomical substrate for digital planning of the chin-support interface. (C) Mesh-based visualization of the support region before digital delimitation and fabrication.

Surface-distance values were calculated in the primary direction from the scanned as-built component to the nominal design surface. This direction was selected because the post-use scan represents the available clinical geometry of the manufactured support.

Complementary nominal-to-scan distances were considered less interpretable because scan coverage, post-processing, surface finishing and post-use artifacts may leave portions of the nominal design surface without complete corresponding scan data. The analysis therefore reports mean absolute distance, root mean square (RMS) distance, median distance, P90/P95 distances, maximum observed distance and the percentage of sampled surface points within predefined 1.0-mm and 2.0-mm thresholds.

These measurements should be interpreted as exploratory CAD-to-as-built surface-deviation descriptors, not as formal regulatory, industrial or certification-level dimensional metrology.

Exploratory CAD-to-as-built surface-deviation metrics of the patient-specific chin-support component. Metric Value Mean absolute surface distance 0.48 mm RMS surface distance 0.62 mm Median surface distance 0.38 mm P90 / P95 surface distance 0.89 / 1.30 mm Maximum observed distance 3.32 mm Surface points within 1.0 mm 92.3% Surface points within 2.0 mm 98.4% Interpretation Exploratory CAD-to-as-built descriptor; not certification-level dimensional metrology Abbreviations: CAD, computer-aided design; RMS, root mean square; P90/P95, 90th and 95th percentile distances.

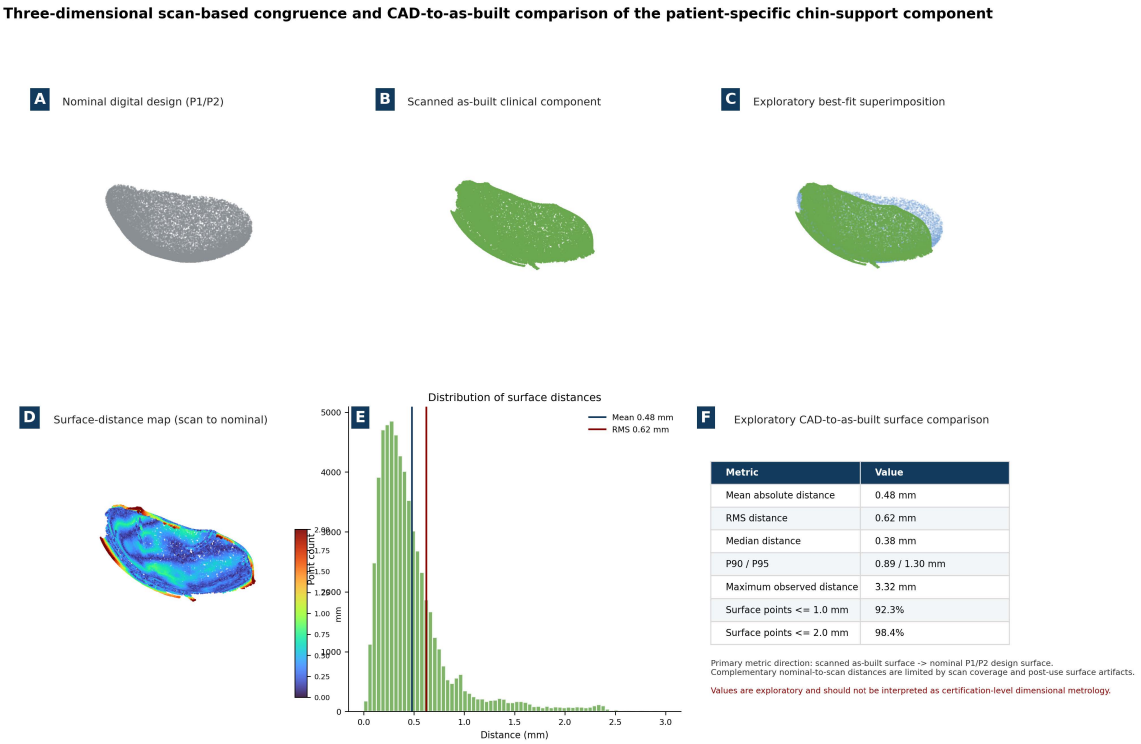
Detailed step-by-step operational controls, including scan acceptance, file conversion, P1/P2 generation, anchorage-channel planning, printing controls, post-processing, data governance, and validation endpoints, are provided in Supplementary Table S1.

Results

Digital fabrication and assembly

The patient-specific Digital Sky Hook framework required three design and printing iterations before the final geometry was standardized for clinical delivery. These iterations were necessary to refine the support contour, marginal extension, wire accommodation, and assembly strategy.

Figure 2 — Exploratory CAD-to-as-built surface-deviation analysis of the patient-specific chin-support interface



Source: Authors' exploratory CAD-to-as-built surface-congruence analysis.
The nominal design geometry derived from the original P1/P2 support components was aligned with the scanned clinically used chin-support component using best-fit/ICP registration. Color-coded surface-distance mapping and summary metrics were used to describe geometric correspondence between the planned and as-built support interface. The analysis should be interpreted as validation-oriented exploratory metrology, not as industrial manufacturing certification. Larger deviations were concentrated near peripheral borders, trimming regions, and wire-accommodation areas, whereas most of the support surface remained within 1.0–2.0 mm of the nominal geometry.

The finalized printed components showed no visible deformation, warpage, or marginal distortion that compromised laboratory assembly or clinical seating. Digital fabrication and assembly The support base was manufactured as separate printed components and subsequently assembled with the metallic framework.

The chromium-nickel wire structure was adapted into the digitally planned negative retention channels, and the printed components were joined with chemically activated acrylic resin. This hybrid workflow preserved the patient-specific geometry of the support interface while maintaining the classical structural logic of the Sky Hook framework.

Clinical seating and soft-tissue tolerance

At clinical delivery, the finalized digital appliance demonstrated passive seating over the mentolabial and symphyseal support area. No hydrocolloid foam, chairside relining, or compensatory comfort material was required to achieve tolerance at the support interface.

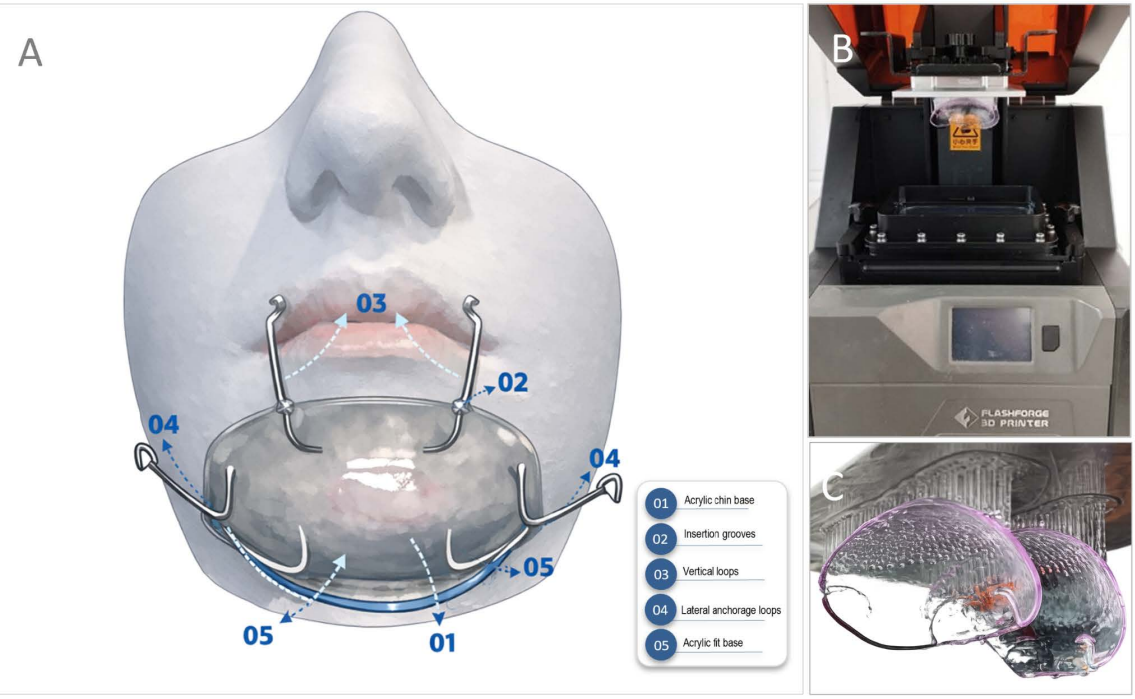
The absence of compensatory lining was considered clinically relevant because padding materials may increase thickness, introduce compressibility, and create an additional source of seating variability.

The identification of the nominal P1/P2 design files allowed the scanned clinically used chin-support component to be evaluated against the original digital design reference.

After exploratory best-fit/ ICP alignment, the primary scan-to-nominal comparison demonstrated a mean absolute surface distance of 0.48 mm and an RMS distance of 0.62 mm. Median distance was 0.38 mm, with P90/P95 values of 0.89/1.30 mm.

In the sampled surface dataset, 92.3% of points were within 1.0 mm and 98.4% were within 2.0 mm of the nominal design reference. The maximum observed distance was 3.32 mm, mainly reflecting peripheral/border regions and scan/post-use surface irregularities rather than uniform central misfit.

Figure 3 — Patient-specific Digital Sky Hook architecture and additive manufacturing



Source: Developed by the authors from the documented design and fabrication workflow.
(A) Schematic representation of the finalized framework, including chin-support base, anterior traction hooks, lateral anchorage arms, and stabilizing framework. (B) DLP additive manufacturing of the customized components. (C) Printed components before final assembly.

This analysis adds a quantitative engineering layer to the workflow. It does not replace formal industrial metrology, because the scan was acquired from a finished and clinically used component.

However, it documents that the manufactured patient-specific support remained close to the nominal design geometry over most of the sampled surface and supports the interpretation of the Digital Sky Hook as an auditable biomechanical support-interface workflow rather than an exclusively narrative clinical fabrication report. The index patient used the appliance for 12 to 14 hours per day over an 8-month clinical-use period.

During follow-up, no clinically relevant soft-tissue adverse events were recorded. Specifically, there were no documented pressure ulcers, persistent erythema, pain requiring discontinuation, device-related tissue injury, or appliance instability that required abandonment of the digital support.

The appliance remained clinically usable during the documented period.

Analog-versus-digital support adaptation

Exploratory comparison between the conventional manually fabricated support and the scan-derived facial reference revealed visible and measurable adaptation discrepancies. When the analog support was positioned against the digital facial model, discrepancies of approximately 2.0 mm at the superior border and 2.5 mm at the inferior border were observed.

These discrepancies were interpreted as compatible with the limitations of analog facial molding and laboratory transfer, including compression of soft tissues during impression taking, cast reproduction error, and manual finishing variability. By contrast, the digital support was derived directly from the patient's non-compressed resting facial topography, thereby bypassing the physical impression and cast-transfer steps.

Abbreviations: CAD, computer-aided design; RMS, root mean square; P90/P95, 90th and 95th percentile distances.

Additional clinical-technical application

A second patient also received a Digital Sky Hook appliance and remained in active use at the time of manuscript preparation. Laboratory and digital-planning documentation confirmed reproducibility of the facial-scan-based support design, component separation, additive manufacturing, wire adaptation, and headcap assembly sequence. Table 3 summarizes the exploratory surface-deviation metrics.

Table 3. Exploratory CAD-to-as-built surface-deviation metrics of the patient-specific chin-support component.

Metric	Value
Mean absolute surface distance	0.48 mm
RMS surface distance	0.62 mm
Median surface distance	0.38 mm
P90 / P95 surface distance	0.89 / 1.30 mm
Maximum observed distance	3.32 mm
Surface points within 1.0 mm	92.3%
Surface points within 2.0 mm	98.4%
Interpretation	Exploratory CAD-to-as-built descriptor; not certification-level dimensional metrology

Source: Authors' exploratory surface-congruence analysis.

Figure 4 — Clinical delivery of the finalized Digital Sky Hook



Source: Authors' clinical archive; de-identified record reproduced with authorization.
(A) Intraoral view showing Class III elastic engagement with the maxillary anchorage unit. (B) Lateral extraoral view after installation, demonstrating the relationship among the chin-support base, anterior hooks, lip clearance, and traction pathway. (C) Frontal view after installation. (D) Inferior view highlighting adaptation of the chin-support interface to the mentolabial and symphyseal region. The finalized appliance demonstrated passive seating without hydrocolloid foam or compensatory lining material.

This second application supported procedural repeatability of the workflow, while the index case remained the primary source for detailed seating assessment, analog-versus-digital comparison, and follow-up interpretation.

Proof-of-concept interpretation

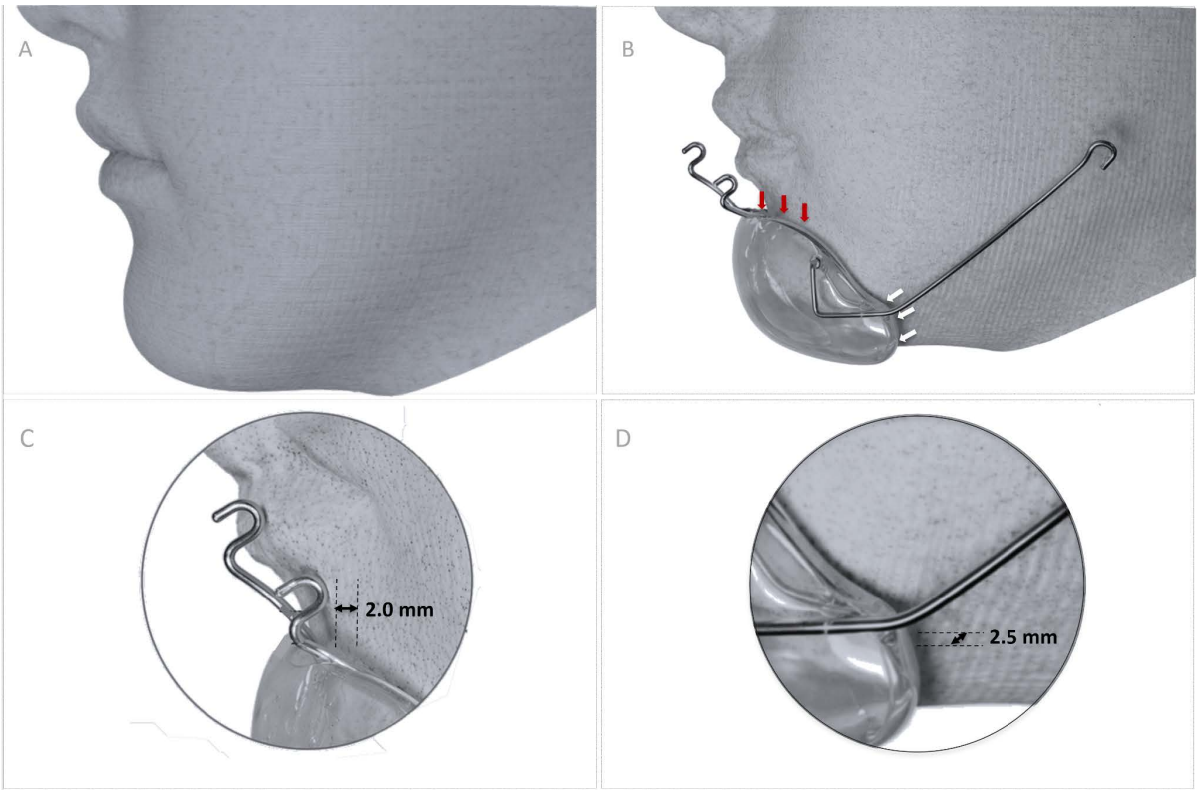
Taken together, the observed results support the feasibility of using non-contact facial acquisition and additive manufacturing to produce a patient-specific chin-supported protraction framework with favorable clinical seating. Within the intended scope of a technical note, the findings demonstrate that digital customization produced a clinically usable support base, eliminated the need for compensatory lining in the index case, and provided an auditable workflow that could be reproduced in a second ongoing-use application.

Discussion

The Sky Hook as a biomechanical interface problem

The present proof-of-concept should be interpreted as a biomechanical interface study. Hickham established the historical mechanical family of chin-supported anterior traction appliances; the present workflow does not replace that lineage. It preserves the classical force architecture and modifies the support-interface pathway through facial surface acquisition, mesh processing, STL-based planning, additive manufacturing, and patient-specific anatomical adaptation[2–6]. This clarification is important because it separates invention, terminology, and improvement.

Figure 5 — Exploratory analog-versus-digital comparison of support adaptation



Source: Authors' clinical and measurement archive; de-identified record reproduced with authorization.
(A) Reference lower facial surface derived from non-contact digital acquisition. (B) Manually fabricated analog support positioned against the scan-derived facial model, showing visible mismatch at the superior and inferior borders. (C) Close-up of the superior discrepancy, measuring approximately 2.0 mm. (D) Close-up of the inferior discrepancy, measuring approximately 2.5 mm. This comparison is descriptive and exploratory and does not constitute formal metrological validation.

Hickham is the historical source of the anterior traction appliance; NOLA/ Hickham is a commercial nomenclature used for prefabricated protraction headgear; Sky Hook is the clinical/geometric descriptor of elevated extraoral hook-based traction; and Digital Sky Hook refers to the digital acquisition, design, fabrication, documentation, and reproducibility of the patient-specific support interface. The term digital is therefore used for the workflow, not to imply that the appliance is electronic or sensorized. The improvement proposed here is not a change in the biological principle of maxillary protraction.

It is a change in the way the force system is seated on the patient. The chin support is part of the force system: its geometry affects seating, wire position, hook orientation, lip clearance, and the stability of the elastic line of action. If the support base is unstable, the intended biomechanics may change even when the same elastic, hook position, and intraoral anchorage are used.

Classical descriptions of Sky Hook therapy already emphasized force balance, hook position, lateral stabilization, patient tolerance, and control of soft-tissue pressure. The present digital workflow keeps these principles but changes how the support interface is obtained: the base is derived from the patient's resting facial surface rather than from a compressed facial impression or a prefabricated morphology. The clinical behavior of a chin-supported protraction appliance depends on whether the support base remains seated during daily use.

During speech, swallowing, mandibular movement, and changes in facial muscle tone, the support interface is repeatedly challenged. A support base that slips, rocks, or compresses localized areas may cause discomfort, reduce adherence, alter the relationship between the anterior hooks and intraoral anchorage, and change the effective moment arm of the traction vector. In this sense, stability is not merely the absence of movement.

It is the preservation of the intended spatial relationship among the chin support, vertical arms, lateral arms, anterior hooks, occipital headcap, intraoral anchorage, and elastic pathway. The Digital Sky Hook attempts to improve this relationship by increasing anatomical congruence between the support base and the patient's mental soft-tissue

contour. The finding that the finalized appliance required no hydrocolloid foam or compensatory lining material is therefore relevant.

It suggests that the support interface was sufficiently congruent to permit clinical use without adding an additional compressible layer between the device and the patient. Padding materials may reduce pain, but they can also mask an inaccurate support base. They increase thickness, introduce deformation under load, and may create variable seating during function.

When an appliance depends on padding to become tolerable, the contact interface becomes less predictable. In the present case, the digital appliance achieved passive seating without compensatory lining, suggesting that the scan-derived support geometry reduced at least one source of mechanical variability.

From analog facial molding to patient-specific digital support

The most important difference between analog and digital workflows occurs at the initial capture of the support anatomy. Conventional facial molding requires physical contact with the lower third of the face and depends on laboratory transfer, acrylic processing, manual delimitation, and freehand finishing. The digital workflow does not necessarily add an entirely new cost layer; rather, it replaces part of an already laboratorial pathway with facial scanning, mesh design, and additive manufacturing.

In settings where facial scanning, biocompatible resin printing, and trained dental/prosthetic laboratories are available, the economic impact is context-dependent and should be evaluated empirically rather than presumed to be prohibitive. Digital facial acquisition reverses this logic. By recording the facial surface without contact and at rest, it allows the support base to be designed from an uncompressed soft-tissue reference.

The digital file then becomes a traceable substrate for design, prototyping, revision, and remanufacturing. This does not make the workflow fully automated or universally reproducible. Operator decisions still influence mesh delimitation, border design, channel placement, wire adaptation, acrylic union, polishing, and clinical adjustment.

However, the digital pathway reduces the dependence on a physically compressed impression and preserves a file-based record of the anatomical interface. The exploratory analog-versus-digital comparison reinforces this argument. The manually fabricated support showed discrepancies of approximately 2.0 mm at the superior border and 2.5 mm at the inferior border when compared with the scan-derived facial model.

These values are descriptive seating indicators rather than formal metrological measurements, because repeated examiner analysis and full three-dimensional deviation mapping belong to the next validation stage. Even so, a 2-mm border mismatch is clinically meaningful when the appliance depends on broad soft-tissue contact, passive seating, and stable hook positioning during prolonged daily wear.

Biomechanical rationale and vector control

The biomechanical importance of the support interface can be understood through the moment relationship M = F x d. In this simplified expression, the generated moment depends not only on the applied force but also on the perpendicular distance between the line of action and the relevant center of resistance or rotation. In clinical maxillary protraction, the exact center of resistance of the maxillary complex cannot be precisely located in vivo and varies according to craniofacial morphology, vertical pattern, maxillary anatomy, and the anchorage configuration. For this reason, the equation should not be treated as a precise clinical measurement in the present report. It is better understood as a conceptual model explaining why changes in the line of action or support position may influence rotational behavior. If the chin support rotates or slides, the position of the anterior hooks changes.

When hook position changes, the elastic pathway and effective moment arm may also change. Thus, even when the clinician selects the correct clinical traction configuration, instability at the support base can alter the delivered mechanics. The lateral wire framework and occipital headcap contribute to the stabilization of this system by counterbalancing excessive displacement of the chin-support assembly and helping preserve lip clearance and support position.

Elastic traction was reported according to configuration and clinical management rather than as a fixed in vivo force value. Although classical Sky Hook mechanics may involve orthopedic forces greater than those used for conventional tooth movement, the actual force delivered by elastics varies with brand, elastic category, degree of elongation, hook-to-hook distance, moisture, fatigue, time in function, and replacement interval. For this reason, the protocol is documented through elastic size, daily replacement, support stability, soft-tissue response, and conceptual biomechanical control, while direct force monitoring is proposed as a future validation endpoint.

Clinical tolerance and soft-tissue safety

Soft-tissue tolerance is not a minor endpoint in extraoral orthopedic therapy. Appliances that require prolonged daily wear must remain acceptable to the patient and safe for the contact tissues. Skin irritation, pressure marks, discomfort, and instability may reduce adherence and compromise the therapeutic plan.

In the present case, the finalized digital appliance was used for 12 to 14 hours per day over an 8-month period without recorded clinically relevant soft-tissue adverse events. This observation supports the feasibility of prolonged clinical use of a patient-specific printed support base under routine follow-up. The absence of compensatory lining material, pressure ulcers, persistent erythema, and pain requiring discontinuation is clinically favorable and supports the hypothesis that anatomical congruence may improve tolerance at the support interface.

Future pressure mapping and patient-reported outcome measures can convert this clinical observation into quantitative evidence. Future studies should transform this clinical observation into measurable endpoints. Thin-film pressure sensors could quantify whether patient-specific support bases reduce localized pressure peaks compared with analog or prefabricated supports.

Patient-reported comfort instruments could measure tolerance and acceptance. Objective wear-time sensors could clarify whether improved seating translates into better adherence. These endpoints are necessary before comfort and compliance can be claimed as reproducible advantages.

What this proof-of-concept shows

This proof-of-concept supports several conclusions within its intended scope. First, a non-contact facial record can be converted into a patient-specific support base for a chin-supported maxillary protraction framework. Second, the digital workflow can preserve a traceable design pathway from facial acquisition to printed support and clinical delivery.

Third, multiple design iterations can be used to refine support geometry before the final clinical appliance is delivered. Fourth, the finalized appliance can achieve passive seating without compensatory lining material. Fifth, an exploratory comparison with an analog support can reveal clinically relevant mismatch at the support borders.

Sixth, the same clinical-technical pathway was reproduced in a second ongoing-use application, supporting procedural repeatability beyond a single fabrication event. These observations are meaningful because they address a specific weakness of conventional fabrication: the instability and distortion of the soft-tissue support interface. The digital workflow improves control over that interface and is scientifically relevant within the scope of a technical note because it converts an operator-dependent analog support stage into a documented, file-based, patient-specific design pathway.

Scope of evidence and future validation pathway

The present article now reports model-based anatomical seating, scan-derived support morphology, procedural repeatability, analog-versus-digital support comparison and exploratory CAD-to-as-built congruence between the nominal P1/P2 design files and the scanned clinically used support component. This additional layer strengthens the manuscript because the support interface is no longer described only by clinical observation or screenshots; it is also documented by a quantitative surface-distance analysis.

This distinction preserves the scientific position of the manuscript. The central claim is that patient-specific digital customization can stabilize, document and audit the chinsupport interface within a structured workflow.

The exploratory CAD-to-as-built results support geometric congruence of the manufactured support but do not establish universal clinical superiority, inter-operator reproducibility or certification-level manufacturing accuracy. This distinction preserves the scientific position of the manuscript.

The central claim is that patient-specific digital customization can stabilize, document, and reproduce the extraoral support interface through which classical protraction mechanics are delivered. This claim is precise, testable, and directly aligned with the evidence presented.

Digital traceability and reproducibility limits

One of the main advantages of the digital workflow is traceability. Original facial files, converted working meshes, intermediate design versions, prototype iterations, final STL files, and manufacturing records can be preserved as discrete steps. This traceability allows retrospective review, remanufacturing, controlled modification, and future comparison across cases.

It also aligns with broader trends in digital health and patient-specific device fabrication, where the value of the workflow is not only the final object but the auditable pathway used to create it. However, traceability should not be confused with full reproducibility. Several steps remain operator-dependent.

The support region must be delineated by a professional. Borders must be designed with clinical judgment. Negative retention channels must be positioned according to the intended wire path.

Wire bending, acrylic union, finishing, polishing, and clinical adjustment remain manual or semi-manual. The workflow is therefore best described as digitally planned, file-based, and potentially reproducible, but not fully automated. This nuance is important.

Overstating reproducibility would invite criticism. A mature digital workflow must identify which steps are standardized and which remain dependent on professional expertise. In the present article, the digital stage standardizes the anatomical support substrate and guides the assembly, while the final orthopedic system still requires orthodontic and laboratory judgment.

Biomaterials and structural considerations

The use of a printed biocompatible resin for a prolonged extraoral support application defines a clear biomaterials validation pathway. The resin used is indicated for surgical-guide applications and was selected from a supplier operating under Anvisa sanitary regulatory authorization (AFE), which supports regulatory traceability of the material pathway. However, prolonged extraoral contact with the menton skin represents a different exposure scenario from intraoperative guide use.

Therefore, AFE status and surgical-guide indication should be understood as regulatory and material-selection safeguards, not as substitutes for device-specific testing of prolonged skin-contact behavior, surface roughness, cleaning stability, cytotoxicity, sensitization risk, or long-term dimensional behavior. The hybrid structure also requires further analysis. The final appliance is not only a printed resin shell.

It is a composite clinical assembly involving printed resin, chromium-nickel wire, acrylic union, finishing, and mechanical loading during use. The interface between resin, wire, and acrylic should be evaluated under cyclic forces, humidity, thermal variation, and repeated insertion/ removal. Fatigue testing is necessary to determine whether the retention channels and acrylic union remain mechanically stable over time. Table 4 summarizes the proposed validation endpoints.

Table 4. What this proof-of-concept supports and the validation endpoints that follow.

Supported by this report	Next validation endpoint
Feasibility of a patient-specific Digital Sky Hook workflow	Prospective comparison with analog and prefabricated support systems
Non-contact acquisition of the support interface	Larger clinical samples with predefined orthopedic and patient-reported endpoints
Passive seating of the final digital appliance	Longitudinal cephalometric or three-dimensional outcome assessment when ethically justified
No need for compensatory lining in the documented case	Long-term follow-up after active protraction
Favorable soft-tissue tolerance during documented use	Thin-film electronic pressure mapping under the chin support
Exploratory analog-versus-digital support discrepancy	CAD-to-print and post-use three-dimensional deviation mapping
File-based traceability of the design workflow	Multicenter workflow reproducibility testing
A structured platform for future validation	Dynamometer-based elastic-force monitoring and finite element analysis
Procedural repeatability documented in a second ongoing-use application	Prospective multi-patient protocols with standardized comfort, adherence, pressure, and outcome endpoints

Source: Authors' synthesis based on the findings of this study and references 1–13.

Validation agenda

The next step is to convert the observed clinical stability, procedural repeatability and exploratory CAD-to-as-built surface-deviation findings into measurable biomechanical endpoints. The validation pathway is summarized in Table 4 and detailed operationally in Supplementary Table S1, including pressure mapping, formal CAD-to-print deviation mapping, direct force monitoring, fatigue testing, finite element analysis and prospective clinical follow-up.

Second, dimensional accuracy should be expanded from the exploratory CAD-to-as-built analysis reported here into formal metrological validation. Future studies should compare final nominal design files with post-processed printed components using controlled scanning protocols, repeated acquisitions, best-fit alignment, color-coded deviation maps, mean absolute deviation, RMS error, maximum deviation, and percentage of surface points within predefined tolerance thresholds.

Third, force behavior should be measured directly.

Inline dynamometers or calibrated tension gauges should record elastic force at working extension, immediately after placement, and after clinically relevant periods of use. These data would prevent misleading reliance on nominal elastic force categories. Fourth, structural durability should be assessed through fatigue testing of the resin-wire-acrylic complex.

Such testing should simulate cyclic loading, moisture, temperature variation, and repeated clinical handling. Fifth, finite element analysis should be used to model stress distribution in the appliance and craniofacial structures. FEA models could explore how facial pattern, support geometry, hook position, elastic vector, and headcap stabilization influence stress concentration and rotational tendency.

Sixth, prospective clinical studies should evaluate patient-centered and orthodontic outcomes. These should include comfort scores, adverse-event monitoring, objective wear-time recording, need for compensatory lining, chairside adjustment burden, and cephalometric or three-dimensional outcomes when clinically justified. Advanced imaging such as CBCT should be reserved for cases in which radiographic acquisition is ethically justified and not performed solely for device validation.

Final interpretation

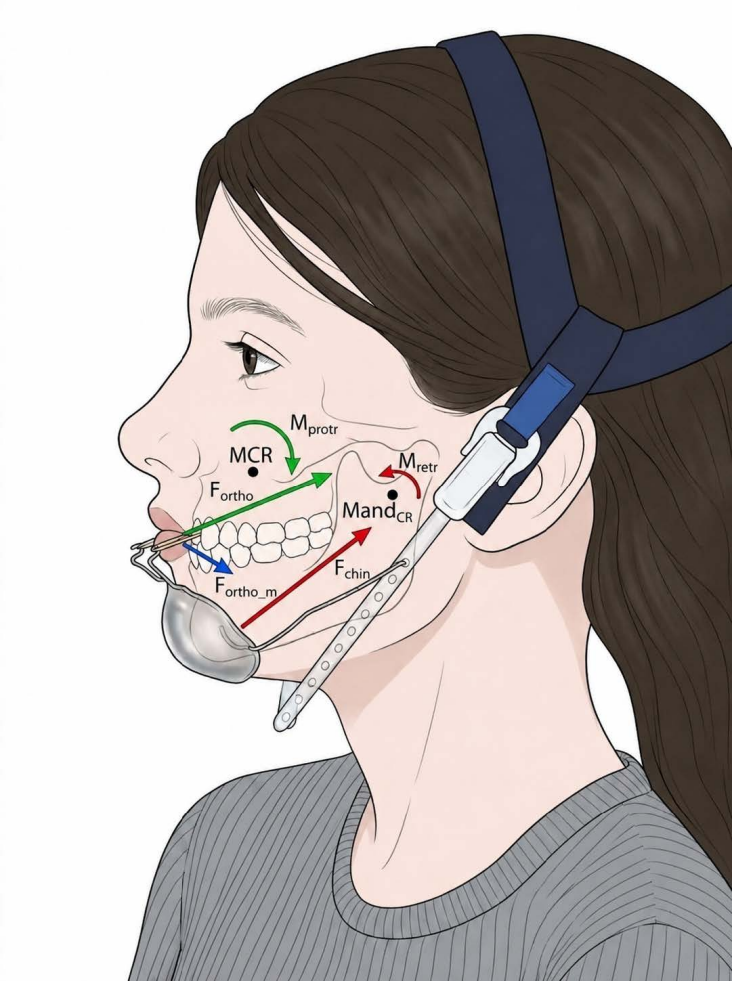
The Digital Sky Hook should therefore be interpreted as a translational platform for patient-specific orthopedic support. Its immediate value lies in stabilizing the support-interface component of a classical maxillary protraction system. Its future value will depend on quantitative studies assessing pressure concentration, adherence, vector geometry, structural behavior, and clinically meaningful orthopedic outcomes.

The article's contribution is specific and clinically relevant: it identifies the support interface as a measurable biomechanical problem and proposes a patient-specific digital method to address it. This reframing can help move chin-supported maxillary protraction from an artisanal appliance-building tradition toward a more auditable, testable, and patient-specific orthopedic device workflow.

Conclusion

This Methods / Technical Note / Validation Study shows that a patient-specific digital workflow can translate classical chin-supported maxillary protraction into a documented, file-based, quantitatively inspectable and clinically deliverable support-interface process. In the index case, non-contact facial acquisition, digital design, additive manufacturing and laboratory assembly enabled fabrication of a customized chin-support base with passive clinical seating, prolonged daily use and no clinically relevant soft-tissue complication during follow-up.

Figure 6 — Conceptual biomechanical rationale of the Digital Sky Hook



Source: Conceptual illustration developed by the authors with AI-assisted image generation under direct human supervision.

The patient-specific chin-support base is designed to improve anatomical congruence and seating stability at the mental soft-tissue interface. The anterior traction pathway links the extraoral hooks to the intraoral maxillary anchorage, while the lateral arms and occipital headcap contribute to stabilization of the extraoral framework. The simplified vector scheme illustrates how changes in force direction and moment arm may influence rotational behavior according to $M = F \times d$. The diagram is conceptual and does not represent direct measurement of in vivo force magnitude, pressure distribution, or center-of-resistance location.

The identification of the nominal P1/P2 design files further allowed an exploratory CAD-to-as-built surface-congruence analysis against the scanned clinical component. The scan-to-nominal comparison showed a mean absolute distance of 0.48 mm, RMS distance of 0.62 mm and 92.3% of sampled surface points within 1.0 mm, supporting geometric coherence between the digital design and the as-built clinical support.

The value of this workflow lies in transforming an operator-dependent analog stage into a traceable, patient-specific, digitally auditable biomechanical interface. Across the two documented clinical-technical applications, the Digital Sky Hook should be interpreted as a translational platform for individualized orthopedic support and as the first evidence layer for future pressure mapping, formal metrology, biomechanical testing and prospective clinical validation.

This work establishes the Digital Sky Hook not merely as a customized orthodontic appliance, but as a digitally engineered, metrically inspectable and clinically deliverable biomechanical interface for chin-supported maxillary protraction.

Required statements

Ethics approval: Formal ethics committee review was not required for this methodological technical note and workflow report according to local institutional requirements. The report was prepared using authorized clinical documentation and de-identified workflow material.

Consent to participate: Written informed consent was obtained from the legal guardian(s) for clinical use of the records and related documentation.

Consent for publication: Written authorization was obtained from the legal guardian(s) for publication of clinical images, diagnostic information, and workflow-related visual material in de-identified scientific form.

Competing interests / intellectual property: The technology described in this manuscript is associated with Brazilian patent application BR 10 2023 008933-0 A2, filed on 10 May 2023 and published on 19 November 2024, entitled "Processo para obtenção de aparelho empregado no tratamento de deficiência maxilar e aparelho." The application lists Lisandro Gonçalves as applicant and Lisandro Gonçalves and Laurindo Zanco Furquim as inventors. The authors declare this intellectual-property relationship transparently. The present manuscript reports clinical and methodological data and does not constitute a commercial endorsement.

Data availability: De-identified workflow and exploratory surface-congruence data are available from the corresponding author on reasonable request, subject to patient privacy, legal guardian authorization, and protection of identifiable facial biometric records.

Digital design file availability: Representative de-identified screenshots, workflow documentation, selected non-identifiable design documentation, and derived measurement outputs can be made available on reasonable request. Original identifiable facial records are not publicly distributed.

Code availability: Not applicable.

AI use disclosure: A generative AI tool was used for language support, grammatical refinement, editorial organization, and the creation of illustrative schematic figures intended solely for scientific communication. AI tools were not used to generate, modify, or design the patient-specific orthopedic device, CAD models, STL files, clinical records, measurements, metrological analyses, or scientific conclusions presented in this manuscript. All technical interpretation, workflow development, engineering decisions, data analysis, and factual responsibility remain solely with the authors.

Editorial declaration: Lisandro Gonçalves serves as Editor-in-Chief of this journal. Editorial handling of this manuscript, including reviewer selection, peer-review oversight, and final decision-making, was conducted independently by the Deputy Editor-in-Chief or another designated independent editor. Lisandro Gonçalves had no role in editorial decision-making for this manuscript.

References

1. Haas AJ. Palatal expansion: just the beginning of dentofacial orthopedics. Am J Orthod. 1970;57(3):219-255. https://doi.org/10.1016/0002-9416(70)90241-1.
2. Hickham JH, inventor. Orthodontic anterior traction appliance. United States patent US 3,401,457. 1968 Sep 17.
3. Hickham JH. The skyhook appliance. Am J Orthod. 1972;62(1):29-41. https://doi.org/10.1016/0002-9416(72)90122-8.
4. Hickham JH. Maxillary protraction therapy: diagnosis and treatment. J Clin Orthod. 1991;25(2):102-113.
5. Furquim LZ. Confecção e instalação do Sky Hook. R Clín Ortodon Dental Press. 2002;1(4):5-13.
6. Gonçalves L, Furquim LZ, Furquim BD, Terada HH. Digital Sky Hook. Clin Orthod. 2023 Dec-2024 Jan;22(6):84-94. https://doi.org/10.14436/2675-486X.22.6.084-094.art.
7. Franchi L, Vichi A, Marti P, Lampus F, Guercio S, Recupero A, et al. 3D printed customized facemask for maxillary protraction in the early treatment of a Class III malocclusion: proof-of-concept clinical case. Materials (Basel). 2022;15(11):3747. https://doi.org/10.3390/ma15113747.
8. Kim H, Kim JS, Kim CS, Becker-Weimann S, Cha JY, Choi SH. Skin irritation in children undergoing orthodontic facemask therapy. Sci Rep. 2023;13(1):2200. https://doi.org/10.1038/s41598-023-29253-0.
9. Thurzo A, Kosnáčová HS, Kurilová V, Surovková J, Moravčíková R, Kováč P, et al. Smartphone-based facial scanning as a viable tool for facially driven orthodontics? Sensors (Basel). 2022;22(20):7752. https://doi.org/10.3390/s22207752.
10. Jindanil T, Zhang B, Seneviratne R, Gredes T, Jamilian A, Volchkevich D, et al. Smartphone applications for facial scanning: a technical and scoping review. Orthod Craniofac Res. 2024;27 Suppl 2:65-87. https://doi.org/10.1111/ocr.12821.
11. Kouhi M, de Souza Araújo IJ, Asa'ad F, Zeenat L, Bojedla SSR, Pati F, et al. Recent advances in additive manufacturing of patient-specific devices for dental and maxillofacial rehabilitation. Dent Mater. 2024;40(4):700-715. https://doi.org/10.1016/j.dental.2024.02.006.
12. Burns NR, Musich DR, Martin C, Razmus T, Gunel E, Ngan P. Class III camouflage treatment: what are the limits? Am J Orthod Dentofacial Orthop. 2010;137(1):9.e1-9.e13. https://doi.org/10.1016/j.ajodo.2009.05.017.
13. Miethke R. John H. Hickham, 1935-2004. Am J Orthod Dentofacial Orthop. 2005;127(1):94. https://doi.org/10.1016/j.ajodo.2004.11.022.

License and reuse

CC BY 4.0

© 2026 Lisandro Gonçalves, Hélio Hissashi Terada. This work is licensed under a Creative Commons Attribution 4.0 International License (CC BY 4.0).
https://creativecommons.org/licenses/by/4.0/

Publisher notice on AI, text and data mining

This article is made available under the Creative Commons Attribution 4.0 International License (CC BY 4.0). Any automated harvesting, large-scale text and data mining, or machine-learning reuse of journal content must preserve proper attribution, source integrity, citation metadata, and compliance with applicable legal, ethical, and platform-use requirements.

Funding: This work received no specific external funding.

Disclosure added on 29 October 2026 following author confirmation; scientific content and conclusions were unchanged.